An image compression method for space multispectral time delay and integration charge coupled device camera*

Li Jin(李 进)[a)b)†], Jin Long-Xu(金龙旭)[b)], and Zhang Ran-Feng(张然峰)[b)]

[a)] *Changchun Institute of Optics, Fine Mechanics and Physics, Chinese Academy of Sciences, Changchun* 130033, *China*
[b)] *Graduate University of Chinese Academy of Sciences, Beijing* 100049, *China*

(Received 27 July 2012; revised manuscript received 11 December 2012)

Multispectral time delay and integration charge coupled device (TDICCD) image compression requires a low-complexity encoder because it is usually completed on board where the energy and memory are limited. The Consultative Committee for Space Data Systems (CCSDS) has proposed an image data compression (CCSDS-IDC) algorithm which is so far most widely implemented in hardware. However, it cannot reduce spectral redundancy in multispectral images. In this paper, we propose a low-complexity improved CCSDS-IDC (ICCSDS-IDC)-based distributed source coding (DSC) scheme for multispectral TDICCD image consisting of a few bands. Our scheme is based on an ICCSDS-IDC approach that uses a bit plane extractor to parse the differences in the original image and its wavelet transformed coefficient. The output of bit plane extractor will be encoded by a first order entropy coder. Low-density parity-check-based Slepian–Wolf (SW) coder is adopted to implement the DSC strategy. Experimental results on space multispectral TDICCD images show that the proposed scheme significantly outperforms the CCSDS-IDC-based coder in each band.

Keywords: multispectral CCD images, Consultative Committee for Space Data Systems – image data compression (CCSDS-IDC), distributed source coding (DSC)

PACS: 42.30.Va **DOI:** 10.1088/1674-1056/22/6/064203

1. Introduction

Multispectral time delay and integration charge coupled device (TDICCD)[1–4] images are of interest for a large number of applications, including geology, environmental monitoring, natural resource management, and meteorology. The growing interest is motivated by several concurring reasons. One of the most important reasons is the improved quality of a state-of-the-art sensor which delivers images with very high spatial, spectral, and radiometric resolution.[5–7] However, together with this wealth of information comes the problem of managing such a huge quantity of data which must be transmitted to the ground station on limited-capacity channels, which takes a long time, and finally disseminated to the end users on common transmission facilities. Therefore, suitable compression algorithms are highly desirable in all the phases of the data lifetime and can play a central role in the successful remote-sensing applications.

Most of the multispectral TDICCD image compression algorithms are based on a three-dimensional (3D) transform stage, such as 3D Karhunen–Loeve transform (3D KLT),[8] 3D discrete cosine transform (3D DCT), and discrete wavelet transform (3D DWT).[9] The 3D DWT provides an efficient way to compress images by separating the multispectral image into several scales in the spatial and temporal dimensions and exploiting the correlations across scales as well as within each scale for intra-bands and inter-bands. There have existed several well-known multispectral image compression algorithms, like 3D EZW,[10] 3D EBCOT,[11] 3D SPIHT, and 3D SPECK.[12] The JPEG2000[13,14] algorithm for a multispectral image in 3D mode, using 3D EBCOT as its kernel, is also a 3D DWT-based compression approach and usually taken as the reference technique. Multi-spectral image compression requires a low-complexity and error-resilient encoder because it is usually completed on board where the energy and memory are limited and transmitted to the ground segment. However, those algorithms based on JPEG2000 and 3D transform that help to provide high compression performance also have excessive implementation complexity.[15] This limits the suitability for satellite-borne missions with high data throughput rates and limited capacities of acquisition, storage, and transmission.

The Consultative Committee for Space Data Systems – Image Data Compression (CCSDS-IDC)[16] specifically targets use aboard spacecraft and focuses more on compression and less on options of handling and distributing compressed data. A careful trade-off has been made between compression performance and complexity, which is very suitable for on-board image compression. However, CCSDS-IDC is only suitable for two-dimensional (2D) remote sensing images and usually does not provide satisfactory results for multispectral data, because it can be employed in each band to reduce spectral redundancy but not reduce spectral redundancy in inter-

*Project supported by the National High Technology Research and Development Program of China (Grant No. 863-2-5-1-13B).
†Corresponding author. E-mail: jinlicareer@yahoo.com.cn
© 2013 Chinese Physical Society and IOP Publishing Ltd

bands.

Given the close spatial and spectral correlation among multi-spectral images, we can employ the distributed source coding (DSC) principle to compress them efficiently at a lower cost. Compared with conventional source coding schemes, the DSC method can shift the complexity from encoder to decoder. A number of the DSC-based compression frameworks have appeared over the past few years. Zhang *et al.*[17] proposed a lossless compression method for multispectral images based on DSC and prediction with very low encoder complexity. Abrardo *et al.*[18] put forth lossless and lossy DSC-based compression methods. However, these methods are not suitable for multispectral TDICCD image compression. In this paper, we propose a low-complexity DSC scheme for onboard compression of multi-spectral images.

The rest of this paper is organized as follows. In Section 2 the DSC theory is introduced. In Section 3 the architecture of the method is presented. In Section 4, the experimental results are demonstrated. In Section 5 some conclusions are drawn from the present study.

2. Distributed source coding theory

In recent years, DSC has received increasing attention from the signal-processing community. Random variables are denoted by capital letters, e.g., X, Y. Realizations of random vectors of finite length n bits are denoted by bold-face lowercase letters, e.g., $\boldsymbol{x}$, $\boldsymbol{y}$. Matrices are denoted by bold-face upper case letters; $\boldsymbol{I}_k$ and $\boldsymbol{Q}_{k_1\times k_2}$ are $k\times k$ identity matrix and $k_1\times k_2$ all-zero matrix, respectively. All variables and channel codes are binary.

Let $\{X_i, Y_i\}_{i=1}^{\infty}$ be a sequence of independent drawings of a pair of independent, identically distributed (IID) correlated random variables (X, Y). It is convenient to model the correlation between X and Y by a "virtual" correlation channel: $X = Y + N$, where the random variable N is the correlation channel noise that is independent of Y.

2.1. Slepian–Wolf coding (SWC)

SWC is concerned with compressing discrete random variables X and Y separately and transmitting the resulting bit-streams over a noiseless channel to the receiver for joint decoding. The Slepian–Wolf theorem[19] asserts that if X and Y are compressed at rates R_X and R_Y, respectively, where $R_X \geq H(X|Y)$, $R_Y \geq H(Y|X)$, and $R_X + R_Y \geq H(X, Y)$, then the joint decoder can recover them nearly without loss. In the sequel, we only focus on the special case, known as source coding with decoder side information, where Y is perfectly known at the decoder as side information. This case can be viewed as approaching the corner point $(R_X, R_Y) = (H(X|Y), H(Y))$ in the Slepian–Wolf rate region.

2.2. Wyner–Ziv coding (WZC)

WZC[20] generalizes the setup of SWC in that coding of X is with respect to a fidelity criterion rather than being lossless. In addition, the source X could be either discrete or continuous. In Ref. [20] there was an examination of the question of how many bits were needed to encode the source X under the constraint that the average distortion between X and decoded version $\hat{X}$ satisfied $E\{d(X,\hat{X})\} \leq D$, on the assumption that the side information Y (discrete or continuous) was available only at the decoder. Denote $R^*_{\mathrm{WZ}}(D)$ as the achievable lower bound of the bit rate for an expected distortion D for WZC, and $R^*_{X|Y}(D)$ as the rate-distortion function of coding X with side information Y available also at the encoder.

2.3. Source-channel coding with decoder side information

When the transmission channel is noisy in the SWC problems, error protection is needed. In the noisy channel SWC case, the separation theorem is proved in Ref. [21] where it is shown that if the receiver has side information Y of the uncoded source X, then the entropy of the source, $H(X)$, in the standard separation theorem is replaced by $H(X|Y)$. Equivalently, the Slepian–Wolf limit in this noisy channel case is $H(X|Y)/C$, where $C \leq 1$ is the channel capacity. A separation theorem for lossy source-channel coding with decoder side information, i.e., the noisy channel WZC case, is given in Ref. [22]. It replaces the conditional entropy $H(X|Y)$ in the separation theorem for noisy channel SWC[21] by the Wyner–Ziv rate-distortion function $R^*_{\mathrm{WZ}}(D)$.

3. Proposed scheme

In terms of the trade-off between memory, complexity, and performance, we present a low-complexity improved CCSDS-IDC (ICCSDS-IDC)-based DSC (ICCSDS-IDC-DSC) scheme for multispectral CCD images consisting of a few bands. Obviously, CCSDS-IDC-based encoders imposed on hardware are less extensive than traditional ones. Furthermore, the proposed ICCSDS-IDC algorithm uses a bit plane extractor to parse the differences in the original image data and its wavelet transformed coefficients. The output of the bit plane extractor will be encoded by a first order entropy coder. This feature provides us with the opportunity to gain image encoders to obtain a better performance than conventional CCSDS-IDC-based encoders and to adopt DSC technique to achieve lower complexity than traditional ones.

3.1. Improved CCSDS-IDC

Figure 1 shows the architecture of the proposed ICCSDS-IDC encoder and decoder.

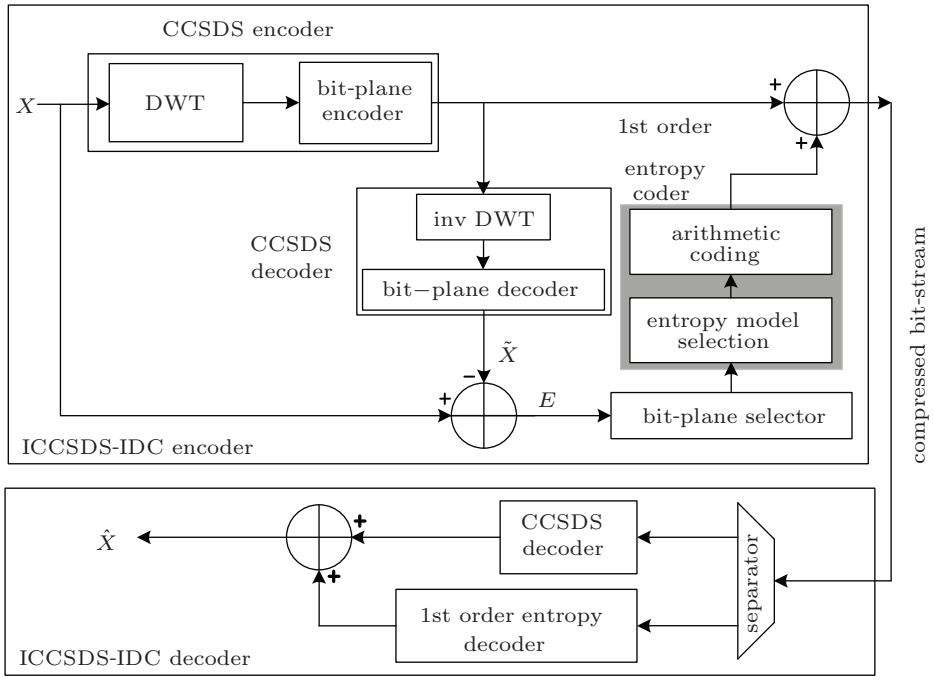


Fig. 1. Proposed ICCSDS-IDC algorithm architecture.

The proposed ICCSDS-IDC combines the CCSDS-IDC algorithm and specific residue image bit plane compensation. The input image X is first encoded by the DWT + BPE and then reconstructed by the decoder to produce the reconstructed image $\tilde{X}$. The residue image E is obtained by subtracting the reconstructed image $\tilde{X}$ from the original image X. The residue image E is further decomposed into bit planes. The specific residue image E will be compressed by 1st order entropy coder to further reduce the volume of data. The encoded bit plane will then be sent together with the CCSDS-IDC compressed image. After receiving the encoded data, the decoder decodes separately the CCSDS-IDC compressed image and the bit plane of residue. The decoded image will be obtained by adding the bit plane to the reconstructed image $\hat{X}$. By applying the bit plane compensation, the proposed ICCSDS-IDC can obtain a higher-quality reconstructed image at a similar bit rate or a similar-quality objective reconstructed image at a lower bit rate. On the other hand, the low complexity makes the proposed algorithm easily implemented.

3.2. Proposed algorithm architecture

Figure 2 shows the proposed ICCSDS-IDC-DSC architecture. We consider the multispectral images consisting of a few bands as a group. In the group, there is a key band which is compressed directly by the ICCSDS-IDC. The key band has a relatively high quality. All the other bands are compressed based on DSC.

The reference bands X_{i-1} and X_{i-2} are transmitted by means of the ICCSDS-IDC. In the ICCSDS-IDC, we combine the CCSDS-IDC and specific residue image bit plane compensation rather than CCSDS-IDC coder. As a result, its reconstructed images $\hat{X}_{i-1}$ and $\hat{X}_{i-2}$ are generated and offered on the decoder side.

In order to make X_i' globally as "similar" to X_i as possible, a second-order filter is adopted and has the following prediction formula:

$$x' = a(v - m_v) + b(w - m_w) + m_x, \tag{1}$$

where "x'" denotes the pixels in the prediction band X_i', "x" the pixels in the current band X_i, "v" and "w" refer to the pixels co-located with the current pixel in two bands X_{i-1} and X_{i-2}, a and b the prediction coefficients, $m_v = E\{v\}$ and $m_w = E\{w\}$ the expectation values of the random variables v and w, respectively. The second-order filter is applied at the encoder to yield an approximate version of X_i. To calculate the prediction coefficients a and b, we use the pixels between X_i, X_{i-1}, and X_{i-2} to fit the data best through solving a Wiener–Hopf equation

$$\begin{bmatrix} \delta_v^2 & \delta_{wv} \\ \delta_{wv} & \delta_w^2 \end{bmatrix} \begin{bmatrix} a \\ b \end{bmatrix} = \begin{bmatrix} \delta_{xv} \\ \delta_{xw} \end{bmatrix}. \tag{2}$$

Define the context windows of the current and the previous band as shown in Fig. 3; the statistical parameters can be approximated as

$$\delta_v^2 = E\{v^2\} - m_v^2 = \frac{1}{M^2}\left(M\sum_{i=1}^{M} v_i^2 - (\sum_{i=1}^{M} v_i)^2\right), \tag{3}$$

$$\begin{aligned} \delta_{wx} &= E\{wx\} - m_w m_x, \\ &= \frac{1}{M^2}\left(M\sum_{i=1}^{M} w_i x_i - \sum_{i=1}^{M} w_i \sum_{i=1}^{M} x_i\right), \end{aligned} \tag{4}$$

where M is the context window size. Other parameters can be calculated likewise.

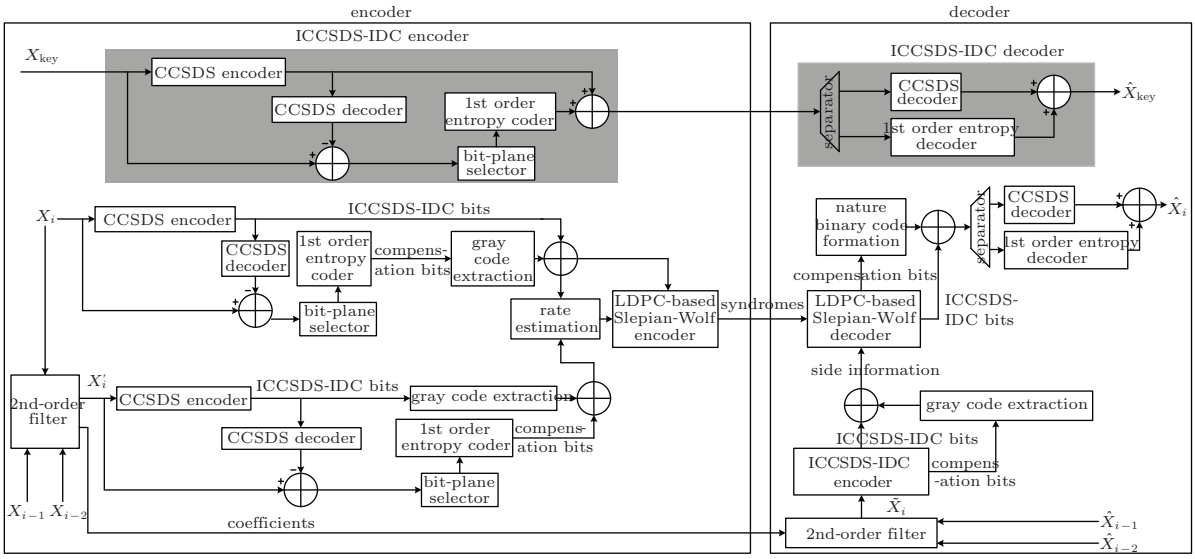


Fig. 2. ICCSDS-IDC-DSC-based coding architecture for multi-spectral images.

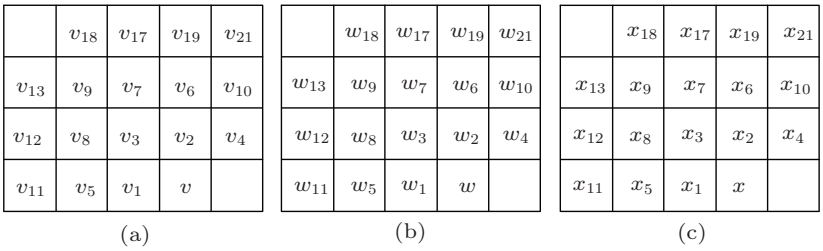


Fig. 3. Definitions of context windows (a) and two previous bands (b), and current band (c).

On the decoder side,

$$\tilde{x}' = a(\hat{v} - m_{\hat{v}}) + b(\hat{w} - m_{\hat{w}}) + m_{\tilde{x}}$$

is adopted as the filter, where $\tilde{x}_i'$ represents the estimated version yielded. Since the second-order model is unknown to the decoder, it is necessary to convey the coefficients a and b to the decoder. The coefficients can help to yield more accurate representation of band X_i, i.e., $\tilde{X}_i'$.

In the case of X_i, DWT transform is introduced, and the bit-planes of the DWT coefficients are extracted and encoded by the BPE algorithm to obtain CCSDS-IDC bit-planes and compressed bits. CCSDS-IDC compressed bits are reconstructed by the decoder to produce the reconstructed image. The residue image is obtained by subtracting the reconstructed image from the original image and further decomposed into compensation bit planes. The compensation bits are gray encoded. In our scheme, we choose LDPC code as the powerful error-correcting code to realize the DSC strategy. The LDPC-based SW coder is implemented to encode the CCSDS-IDC bits. The essential parameter that determines the compression rate is the value of crossover probabilities (the crossover probabilities between the corresponding bit-plane locations of X_i and X_i', with BSC being the virtual channel), and it is the key ingredient of the LDPC-based SW encoder. The ICCSDS-IDC encoder is used to process the DWT coefficients of X_i' in order to extract CCSDS-IDC and compensation bit-planes. These generated CCSDS-IDC and compensation bits are compared with those of X_i so as to compute the crossover probabilities. Additionally, a table is built offline that relates different crossover probabilities to compression rates, at both the encoder and the decoder. Once the crossover probability is obtained, a proper compression rate can be selected. Specifically, we use the LDPC accumulate (LDPCA) code[23] to implement the SW encoder.

The structure on the right side shows how it works at the DSC decoder. The estimated value $\tilde{X}_i'$ is generated by directly using $\hat{X}_{i-1}'$ and $\hat{X}_{i-2}'$. Then, the ICCSDS-IDC and compensation bits of $\tilde{X}_i'$ are obtained by the ICCSDS-IDC encoder and then made available as side information. Combined with the precise side information and the passed syndromes, the LDPC-based SW decoder is then employed to reconstitute the ICCSDS-IDC bits. Afterward, the compensation bits in gray code are transformed to natural binary code. After the CCSDS and the first order entropy decoder, we finally reproduce the band $\hat{X}_i$.

4. Experimental results

4.1. Compression efficiency

As usually done in the literature, we use three groups 512×512, 8 bpp (bits per pixel) remote sensing images with four bands to measure the radiation from the Earth filtered at wavelengths 0.45 μm–0.52 μm, 0.52 μm–0.60 μm, 0.63 μm–0.69 μm, and 0.76 μm–0.90 μm, for evaluating our ICCSDS-IDC-based DSC scheme. Three-level Daubechies 9/7 DWT is performed. LDPCA code with a length of 396 specified in Ref. [23] is used, which can perform within 10% of the SW bound at a moderate rate. All software is written in MATLAB, and runs on PCs with 3.6-GHz CPU and 4-GB memory. The following diagrams illustrate the results.

Figure 4 shows the key bands for three original and reconstructed images. The code rate of the key bands is 2.0 bpp.

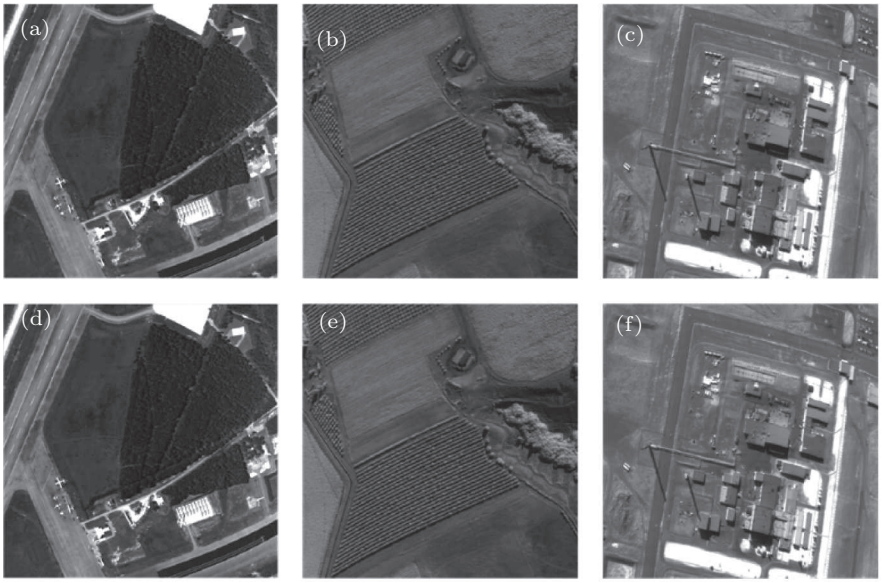


Fig. 4. Key band images : original image ((a)–(c)) and reconstructed image at 2.0 bpp ((d)–(f)).

To objectively evaluate the performance of the proposed DSC scheme, extensive experiments are carried out on a number of multi-spectral data at various coding bit-rates. In the first experimental part, we compare the compression results obtained with the proposed coder with those achieved with 2D SPIHT,[24] JPEG2000,[25] CCSDS,[26] and JPEG-LS[27] independently. The quality assessment of the decoded images is based on rate-distortion results measured by the overall SNR and given by

$$\mathrm{PSNR} = 10\log_{10}\left(\frac{P}{\mathrm{MSE}}\right)\ (\mathrm{dB}), \tag{5}$$

where P and MSE denote the power of the original image and the mean squared error, respectively. Figure 5(a) shows the test results of PSNR at 2.0 bpp, 1.0 bpp, 0.5 bpp, and 0.25 bpp using our method. The PSNR comparisons are demonstrated in Fig. 5(b). Due to fully using intra- and inter-redundancy of DWT coefficients, the proposed ICCSDS-IDC-based DSC scheme achieves the best compression performance and 1.225-dB∼8.197-dB PSNR gain on average in comparison with the other five DSC-based codes in norm compression ratio 1 bpp.

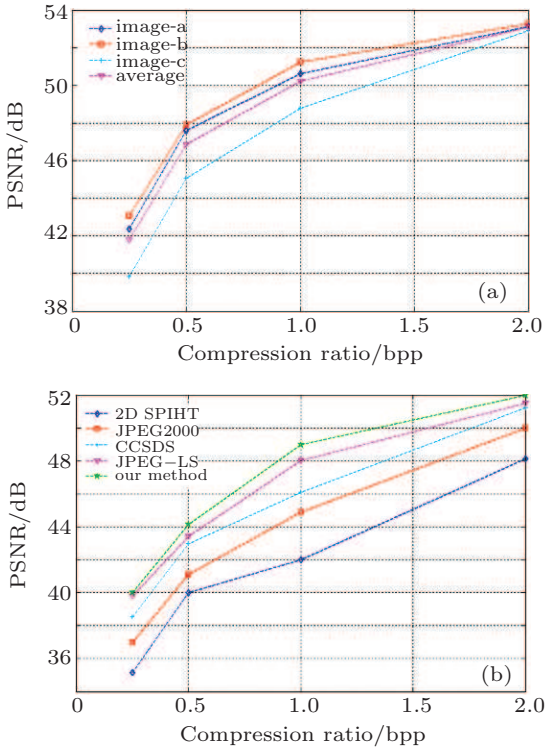


Fig. 5. (color online) The test results of PSNR at 2.0 bpp, 1.0 bpp, 0.5 bpp, and 0.25 bpp.

4.2. Complexity

The complexity of the proposed algorithm is compared with those of existing schemes. As a global complexity measure, we take the running time of a software implementation of the encoders, in C language, on Windows workstation and then the C software is optimized and runs a TMS320DM642 EVM board. The results are reported in Table 1 and are normalized with respect to the complexity of 3D-SPIHT. As can be seen, our proposed algorithm is faster than 3D-SPIHT while providing better compression performance.

Table 1. Complexity of various encoders.

Algorithm	Complexity	Throughput
3D-SPIHT	1	27 ksample/s
JPEG-LS	0.89	115 ksample/s
DWT-based DSC	0.71	189 ksample/s
Our method	0.52	290 ksample/s

There is a key reason why our scheme can achieve a better performance than others. First, the gray code is used to enhance the correlation between the source and the side information. The DSC coder can achieve better coding efficiency with more accurate side information. We can employ the close relation of the multi-spectral images in our scheme more effectively than in others. Overall, the proposed scheme shows excellent lossy compression performance and delivers better compression results than the commonly used coders while exhibiting low computational complexity.

5. Conclusion

In this paper, we propose a low-complexity ICCSDS-IDC-based distributed source coding (DSC) scheme for multispectral TDICCD image consisting of a few bands. Our scheme is based on an ICCSDS-IDC approach that uses a bit plane extractor to parse the differences in the original image and its wavelet transformed coefficients. The output of bit plane extractor will be encoded by a 1st order entropy coder. A low-density parity-check-based Slepian–Wolf (SW) coder is adopted to implement the DSC strategy. Experimental results on space multispectral TDICCD images show that the proposed scheme considerably outperforms the DWT-based coder in each band.

References

[1] Li J, Jin L X, Li G N and Zhang Y 2012 *J. Electron. & Inf. Technol.* **34** 1248
[2] Wang D J and Zhang T 2011 *Chin. Phys. B* **20** 087202
[3] Li J, Jin L X, Li G N, Zhang K and Wang W H 2012 *Spectroscopy and Spectral Analysis* **32** 1700
[4] Qiao N S and Zou B J 2013 *Chin. Phys. B* **22** 014203
[5] Li J, Jin L X, Li G N, Zhang K, Wang W H, Zhang R F and Zhu P 2012 *Journal of Optoelectronics: Laser* **23** 866
[6] Zhang X, Zheng Y G and Zhang H J 2006 *Chin. Phys.* **15** 2185
[7] Li J, Jin L X, Han S L, Li G N and Wang W H 2012 *Optics and Precision Engineering* **20** 1090
[8] Ian B and Joan S S 2010 *IEEE Trans. Geosci. Remote Sens.* **487** 2854
[9] Amar A 2011 *Journal of Display Technology* **711** 586
[10] Jerome M S 1992 *IEEE International Conference on Acoustics, Speech and Signal Processing*, March 23–26, 1992, Princeton, USA p. 657
[11] David T 2000 *IEEE Trans. Image Process.* **97** 1158
[12] Tang X L and William A P 2006 *Hyperspectral Data Compression* (New York: Springer-Verlag) p. 273
[13] David S T and Michael W M 2002 *JPEG*2000*: Image Compression Fundamentals, Standards, and Practice*, 2nd edn. (New York: Springer) p. 101
[14] Wang X Y, Yun J J and Zhang Y L 2011 *Chin. Phys. B* **20** 104203
[15] Pan W, Zou Y and Ao L 2008 *Proceedings of* 2008 3*rd International Conference on Intelligent System and Knowledge Engineering*, November 17, 2008, Xiamen, China, p. 1237
[16] CCSDS 2005 *Image Data Compression* (CCSDS-122.0-B-1 Blue Book) (Washington, DC: CCSDS) p. 11
[17] Zhang J, Li H and Chen C W 2009 *Proc. ICME*, July, 2009, New York, p. 141
[18] Andrea A, Mauro B, Enrico M and Filippo N 2010 *IEEE Trans. Geosci. Remote Sens.* **484** 1892
[19] Slepian J and Wolf J 1973 *IEEE Trans. Inf. Theory* **19** 471
[20] Wyner A and Ziv J 1976 *IEEE Trans. Inf. Theory* **22** 1
[21] Shamai S and Verdu S 1995 *Eur. Trans. Telecommu.* **6** 587
[22] Shamai S, Verdu S and Zamir R 1998 *IEEE Trans. Inf. Theory* **44** 564
[23] David V, Anne A and Bernd Girod 2005 *Proc.* 39*th Asilomar Conf. Signals, Syst. Comput.* November 1, 2005, Pacific Grove, CA, p. 1203
[24] Jin Y and Lee H J 2012 *IEEE Transactions on Circuits and Systems for Video Technology* **227** 1064
[25] Kishor S and Swapna B 2011 *IEEE Transactions on Circuits and Systems for Video Technology* **216** 825
[26] Jose E S, Estanislau A, Josep S, Ian B, Joan S S and Aaron K 2011 *First International Conference on Data Compression, Communications and Processing*, June 21–24, 2011, Palinuro, p. 222
[27] Xie Y and Jing X 2009 *Network Infrastructure and Digital and Content Conference*, November 6–8, 2009, Beijing, China, p. 353